Study of a Penning Trap

Aline Rangøy Brunvoll, Even Tobias Eriksen and Vilde Ung
(Dated: October 24, 2022)

We studied the behaviour of charged particles inside a Penning trap by simulating the movement of particles in an electric and magnetic field. This was achieved by solving the equations of motion for each particle using both the fourth-order Runge-Kutta (RK4) method and the forward Euler (FE) method implemented in `C++`. The estimated error rate of RK4 was 4.0 and 1.446 for FE. By running simulations both with and without particle interaction, we saw that the movement of non-interacting particles followed a stable pattern of oscillating movement, while the interacting particles had a more unpredictable trajectory. We also studied the resonance of the system by simulating a time-dependent electric field and examining the amount of particles remaining in the Penning trap after 500 µs. We observed resonance for frequencies in the range $\omega_V \in (1.35, 1.4)$MHz, both with and without particle interactions.
GitHub repository: https://github.com/ungvilde/FYS4150/tree/main/Project%203

I. INTRODUCTION

A *Penning trap* is a device that traps and stores electrically charged particles by inducing a static configuration of electric and magnetic fields. This allows the user to isolate and study single particles within a confined space. At CERN, Penning traps are used to control and confine anti-matter particles to be studied in various experiments [1]. Penning traps can also be used for confirming the Standard model, for instance in determining fundamental constants [2, p. 3]. Figure 1 shows how a Penning trap can be configured.

In this article, we study the behaviour of positively charged particles inside an ideal Penning trap. We will focus on how the electric and magnetic fields of the trap, as well as the fields induced by the charged particles themselves, affect the particles' movement in the physical space and the phase space. The three-dimensional movement of the particles can be described using a set of differential equations that are quite complicated to solve analytically, and we will therefore solve them numerically using a self-written `C++` program. A model of our own allows us to simulate the system in greater detail and gain more insight about its statistical properties. We then simulate the movement of particles in a Penning trap while varying the different parameters of the system. We explore how factors, such as particle interactions and time-varying potential, affect the particle trajectories and resonance phenomena.

In Section II, we introduce the analytical expressions and numerical methods we need in order to simulate the movement of charged particles in an electromagnetic field. Section III presents the figures and results that are most relevant to our study of the ideal Penning trap. In Section IV, we analyse the figures and consider the physical implications of our results, as well as the validity of our computations. Finally, Section V provides a brief review of the numerical experiments we performed and our key results.

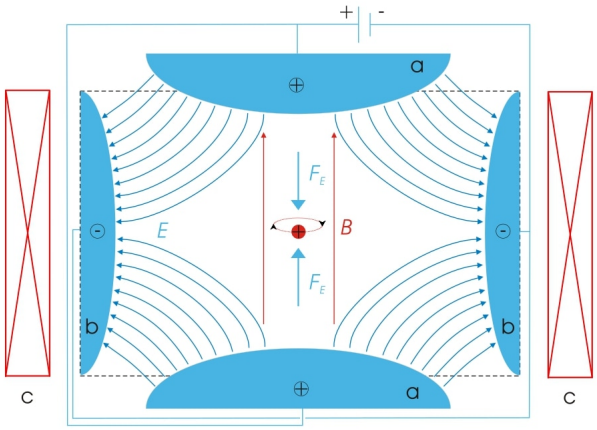

Figure 1. Schematic of a Penning trap. (a) denotes the two positive end cap electrodes and (b) shows a cross-section of the negatively charged ring electrode. The blue arrows denote the electric field generated by the three electrodes, and is overlain by a magnetic field in the z-direction, which is set up by the two cylindrical magnets (c) (where only the cross-section is shown). This illustration is by Arian Kriesch, taken from [3].

II. METHODS

A. The ideal Penning trap

As mentioned, the main function of the Penning trap is to confine charged particles and make sure they stay inside a space outlined by a static electric- and magnetic field. An illustration of such a system is given in Figure 1. This illustration is a cross section of a Penning trap. There are three electrodes in a Penning trap. The one at the top and the one at the bottom are positively charged and marked by a in the illustration. We call these the end caps of the trap. The third electrode is a negatively charged ring encircling the area between the a-electrodes and is marked with b in the illustration.

This configuration sets up a strong electric field going from the positively charged electrodes to the negatively charged ring, marked by blue arrows in the illustration.

The generated electric field can only restrict the particles movement in the z-direction. For the Penning trap to work it needs a static magnetic field applied in the z-direction, marked by red arrows pointing upwards in the illustration. A particle will then start to gyrate within the boundaries of the magnetic field.

B. Electrodynamics and classical mechanics

From Maxwell's equations we can write the static electric field as a gradient of the electric potential V. This can be expressed as

$$\mathbf{E} = -\nabla V, \tag{1}$$

where the electric potential for our ideal Penning trap is given as

$$V(x, y, z) = \frac{V_0}{2d^2}(2z^2 - x^2 - y^2). \tag{2}$$

Here, V_0 is the potential applied to the electrodes and $d = \sqrt{z_0^2 + r_0^2/2}$ is the *characteristic dimension*, where z_0 denotes the distance from the center of the Penning trap to the end caps and r_0 is the distance from the center to the ring. We will also consider the case where the potential varies with time, by doing the replacement

$$V_0 \leftarrow V_0[1 - f\cos(\omega_V t)]. \tag{3}$$

Here, f is the amplitude and ω_V is the angular frequency.

The electric field traps the charged particle in the z-direction, but still allows movement in the (x, y)-plane. In order to keep the particle trapped in the (x, y)-plane and restrict the gyration radius, a sufficiently strong homogeneous magnetic field $\mathbf{B}$ is set up in the z-direction. We will set our static magnetic field to be

$$\mathbf{B} = B_0\hat{e}_z = (0, 0, B_0), \tag{4}$$

where B_0 is the field strength.

Charged particles set up electric fields of their own that interact with each other. Using Coulomb's law, we define this interaction in a static electric field as

$$\mathbf{E} = k_\mathrm{e}\sum_{j=1}^{n} q_j \frac{\mathbf{r} - \mathbf{r}_j}{|\mathbf{r} - \mathbf{r}_j|^3}, \tag{5}$$

where $k_\mathrm{e} = 8.9876 \cdot 10^9$ kg m^3 s^{-4} A^{-2} is Coulomb's constant. The electric field $\mathbf{E}(\mathbf{r})$ given at a point $\mathbf{r}$ is set up by the point charges $\{q_1, ..., q_n\}$, distributed at points $\{\mathbf{r}_1, ..., \mathbf{r}_n\}$. This will also be referred to as Coulomb interaction.

The force exerted on each particle due to the electric and magnetic fields is called the *Lorentz force* and is given as

$$\mathbf{F} = q\mathbf{E} + q\mathbf{v} \times \mathbf{B}, \tag{6}$$

where q is the electric charge of the particle and $\mathbf{v}$ is its velocity.

In a uniform magnetic field, where all other forces are absent, charged particles will experience a constant acceleration due to the Lorentz force and will start to move in a circle around a guiding center. This can be seen in the middle of Figure 1. The movement will be in the plane perpendicular to the magnetic field direction. Negative charged particles will rotate counterclockwise and positive charged particles will rotate clockwise. The movement of the particles are visualized in Figure 15.

If we add an electric field perpendicular to the magnetic field pointing downwards, the guiding center of the particles will start to drift. This means that the particles will begin to move in one direction while they gyrate around the guiding center.

C. The equations of motion

For a single particle inside the Penning trap, the equations of motion are given by

$$\ddot{x} - \omega_0\dot{y} - \frac{1}{2}\omega_z^2 x = 0 \tag{7}$$

$$\ddot{y} + \omega_0\dot{x} - \frac{1}{2}\omega_z^2 y = 0 \tag{8}$$

$$\ddot{z} + \omega_z^2 z = 0, \tag{9}$$

where $\omega_0 \equiv qB_0/m$ and $\omega_z^2 \equiv 2qV_0/md^2$. The equations in the x- and y-directions are coupled and need to be written as a single differential equation in order to solve them. By defining the complex function $f(t) = x(t) + iy(t)$ we find that the single differential equation made up of (7) and (8) can be written as

$$\ddot{f} + i\omega_0\dot{f} - \frac{1}{2}\omega_z^2 f = 0, \tag{10}$$

where $\ddot{f}$ and $\dot{f}$ are time-derivatives. The general solution to this equation is

$$f(t) = A_+ e^{-i(\omega_+ t + \phi_+)} + A_- e^{-i(\omega_- t + \phi_-)}, \tag{11}$$

where ϕ_+, ϕ_- are constant phases and A_+, A_- are positive amplitudes. $\omega_\pm$ is given by

$$\omega_\pm = \frac{\omega_0 \pm \sqrt{\omega_0^2 - 2\omega_z^2}}{2}. \tag{12}$$

The general solution to equation (9) is much simpler to find, as it is already a single differential equation. The general solution is given as

$$z(t) = A + Be^{-\omega_z^2 t}, \tag{13}$$

where A and B are constants. The detailed derivation of equations (7) - (13) can be found in Appendix A.

We also want to simulate the Coulomb interactions between charged particles. For this we need the following equations of motion:

$$\ddot{x}_i - \omega_{0,i}\dot{y}_i - \frac{1}{2}\omega_{z,i}^2 x_i - k_e \frac{q_i}{m_i}\sum_{j\neq i} q_j \frac{x_i - x_j}{|\mathbf{r}_i - \mathbf{r}_j|^3} = 0$$
$$\ddot{y}_i + \omega_{0,i}\dot{x}_i - \frac{1}{2}\omega_{z,i}^2 y_i - k_e \frac{q_i}{m_i}\sum_{j\neq i} q_j \frac{y_i - y_j}{|\mathbf{r}_i - \mathbf{r}_j|^3} = 0$$
$$\ddot{z}_i + \omega_{z,i}^2 z_i - k_e \frac{q_i}{m_i}\sum_{j\neq i} q_j \frac{z_i - z_j}{|\mathbf{r}_i - \mathbf{r}_j|^3} = 0,$$

where the constants ω_z and ω_0 are the same as for the single-particle equations of motion. As these expressions are much more complex than the case for a single particle, we will not solve them analytically, but rather solve them numerically. The equations are taken from [1].

For evaluating our numerical solutions, a specific analytical solution is in order. We will consider a single charged particle with the initial conditions $x(0) = 0$, $\dot{x}(0) = 0$, $y(0) = 0$, $\dot{y}(0) = v_0$, $z(0) = z_0$ and $\dot{z} = 0$. This gives us the specific solutions

$$x(t) = \mathrm{Re}\{f(t)\}$$
$$y(t) = \mathrm{Im}\{f(t)\}$$
$$z(t) = z_0 \cos(\omega_z t),$$

and

$$A_+ = \frac{v_0 + \omega_- x_0}{\omega_- - \omega_+},$$
$$A_- = -\frac{v_0 + \omega_+ x_0}{\omega_- - \omega_+},$$
$$\phi_+ = 0, \quad \phi_- = 0,$$

for equation (11). The specific solutions are given in [1].

As shown in Appendix A, we can write the upper and lower bounds of the particle's distance from the origin as

$$R_+ = A_+ + A_- \tag{14}$$
$$R_- = |A_+ - A_-|. \tag{15}$$

D. Algorithms and errors

We use the 4th-order Runge-Kutta method (RK4) for the numerical experiments. Let

$$\frac{\mathrm{d}y}{\mathrm{d}t} = f(t, y),$$

denote the first-order differential equation that we want to solve, with initial condition $y(t_0) = y_0$. RK4 is a method based on approximating higher order derivatives by numerical differences. That is, we evaluate f at four different points, and use these values to approximately reproduce the Taylor series [4, p. 301]. The RK4 method involves computing

$$k_1 = hf(t_i, y_i)$$
$$k_2 = hf(t_i + h/2, y_i + k_1/2)$$
$$k_3 = hf(t_i + h/2, y_i + k_2/2)$$
$$k_4 = hf(t_i + h, y_i + k_3),$$

where $h > 0$ is a small number denoting the step size along the time axis. Applying Simpson's rule yields

$$y_{i+1} = y_i + \frac{1}{6}(k_1 + 2k_2 + 2k_3 + k_4). \tag{16}$$

Here, y_{i+1} is the numerical estimate of $y(t_i + h)$, which is based on the current value y_i. The k_1 value gives us the slope at a time t_i, as in Euler's method. The k_2 value calculates the slope at the midpoint to predict $y_{i+1/2}$. The k_3 value further improves the slope of $y_{i+1/2}$. For computing k_4 we use the predicted slope found by k_3 to predict the value of y_{i+1}. Finally, we predict the value of y_{i+1} with (16).

RK4 is a fourth-order method, which means that the global truncation error is of the order $\mathcal{O}(h^4)$ [5, p. 252].

The RK4 method is used for solving first-order differential equations, while the equations of motion that we consider are second-order differential equations. We therefore reformulate the equations of motion in terms of two coupled first-order differential equations. That is, we use RK4 to solve

$$\dot{\mathbf{v}} = \frac{\mathbf{F}}{m} \tag{17}$$
$$\dot{\mathbf{r}} = \mathbf{v}. \tag{18}$$

The details of our implementation of RK4 with first-order coupled differential equations can be seen in Algorithm 1.

To verify the results from the RK4 method, we use a modified version of the forward Euler method, known as the Euler-Cromer method. We refer to this method as FE in the report. Given a pair of coupled differential equations

$$\frac{\mathrm{d}v}{\mathrm{d}t} = a(t), \quad \frac{\mathrm{d}x}{\mathrm{d}t} = v(t), \tag{19}$$

with $a(t) = a(x(t), v(t), t)$ and initial conditions $x(t_0) = x_0$ and $v(t_0) = v_0$. The Euler-Cromer method can be written as

$$v_{i+1} = v_i + ha_i$$
$$x_{i+1} = x_i + hv_{i+1}.$$

Note that we use v_{i+1} to evaluate x_{i+1}. This is a first-order method, with a global truncation error of the order $\mathcal{O}(h)$ [5, p. 247].

We want to estimate the error convergence rate for both FE and RK4. To compute this estimate, we use

$$r_{\mathrm{err}} = \frac{1}{3}\sum_{k=2}^{4} \frac{\log(\Delta_{\max,k}/\Delta_{\max,k-1})}{\log(h_k/h_{k-1})}, \tag{20}$$

Algorithm 1 Evolve one time step using fourth-order Runge-Kutta algorithm for coupled differential equations.

$v_i \leftarrow$ Velocity of particle i at time t
$r_i \leftarrow$ Position of particle i at time t
$N \leftarrow$ Num. particles in Penning trap
$v_{\text{init}} \leftarrow v$
$r_{\text{init}} \leftarrow r$ ▷ Temporary copies of positions and velocities of particles in Penning trap at time t
for $i = 1, \ldots, N$ **do**
  $F_i \leftarrow$ Force on particle i ▷ Depends on position, particle interaction, and if **E** is time-dependent.
  $k_{v1,i} \leftarrow h \cdot F/m$
  $k_{r1,i} \leftarrow h \cdot v_i$
for $i = 1, \ldots, N$ **do** ▷ Now loop through the particles to update position and velocity.
  $r_i \leftarrow r_{\text{init},i} + 0.5k_{r1,i}$
  $v_i \leftarrow v_{\text{init},i} + 0.5k_{v1,i}$
for $i = 1, \ldots, N$ **do**
  $k_{v2,i} \leftarrow h \cdot F_i/m$
  $k_{r2,i} \leftarrow h \cdot v_i$
for $i = 1, \ldots, N$ **do**
  $r_i \leftarrow r_{\text{init},i} + 0.5k_{r2,i}$
  $v_i \leftarrow v_{\text{init},i} + 0.5k_{v2,i}$
for $i = 1, \ldots, N$ **do**
  $k_{v3,i} \leftarrow h \cdot F_i/m$
  $k_{r3,i} \leftarrow h \cdot v_i$
for $i = 1, \ldots, N$ **do**
  $r_i \leftarrow r_{\text{init},i} + k_{r3,i}$
  $v_i \leftarrow v_{\text{init},i} + k_{v3,i}$
for $i = 1, \ldots, N$ **do**
  $k_{v4,i} \leftarrow h \cdot F_i/m$
  $k_{r4,i} \leftarrow h \cdot v_i$
for $i = 1, \ldots, N$ **do** ▷ Now we do a final update of the positions and velocities.
  $r_i \leftarrow r_{\text{init},i} + \frac{1}{6}(k_{r1,i} + 2k_{r2,i} + 2k_{r3,i} + k_{r4,i})$
  $v_i \leftarrow v_{\text{init},i} + \frac{1}{6}(k_{v1,i} + 2k_{v2,i} + 2k_{v3,i} + k_{v4,i})$

where $\Delta_{\text{max,k}} = \max_i |\mathbf{r}_{i,\text{exact}} - \mathbf{r}_i|$ is the maximum error of the simulation with stepsize h_k. We base the estimate on four different values of h_k.

III. RESULTS

In the numerical experiments we performed, the Penning trap had constant electric field with potential $V_0 = 25.0\,\text{mV}$ unless otherwise specified, and constant magnetic field with strength $B_0 = 1.0\,\text{mV}$ in the z-direction. The characteristic distance was set to $d = 500\,\mu\text{m}$. We simulated calcium ions (Ca^+), which have charge $q = 1\,e$ and atomic mass $m = 40.078\,\text{u}$. We used the fourth order Runge-Kutta method to perform the numerical experiments, unless otherwise specified.

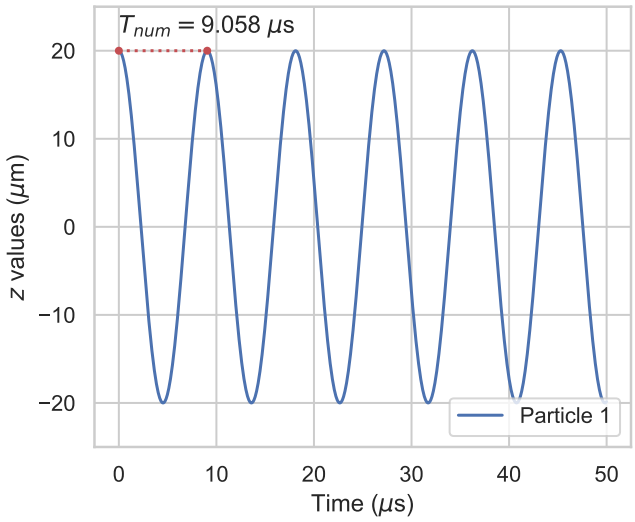

Figure 2. Plot of the z values for a single particle as a function of time. The red dotted line denotes the period of the oscillations, given by $T_{\text{num}} = 9.058\,\mu\text{s}$.

A. Single-particle experiments

We simulated a single particle with initial position $(20, 0, 20)\mu\text{s}$ and velocity $(0, 25, 0)\mu\text{m}/\mu\text{s}$ in a Penning trap for $50\,\mu\text{s}$. We will refer to this specific particle instance as Particle 1. In this case, we can use the specific analytic solution presented in Section II for comparison. For the experimental setup we used, the angular frequency in the z-direction is given by

$$\omega_z = \sqrt{\frac{2 \cdot 2.41 \cdot 10^6}{40.078 \cdot 500^2}} = 0.694\,\text{rad}/\mu\text{s}, \tag{21}$$

which gives a period of $T = 9.059\,\mu\text{s}$. Comparing this to the results in Figure 2, we see that the numerical solution agrees with the analytic solution. The period of the numerical solution was $T_{\text{num}} = 9.058\,\mu\text{s}$.

We further explored how the numerical solutions compared to the analytic solution for both RK4 and FE. With both methods, we simulated Particle 1 for $50\,\mu\text{s}$ using different numbers of time steps, which corresponds to different step sizes along the time axis. Specifically, we used $N_1 = 4.000$, $N_2 = 8.000$, $N_3 = 16.000$ and $N_4 = 32.000$, which corresponds to step sizes of $dt = 50/N_k\mu\text{s}$. We plotted the relative error of each method with a given N_k as a function of time. The results for FE can be seen in Figure 3, and the results for RK4 can be seen in Figure 4. Using (20), we estimated the convergence rate of each method. The results can be seen in Table I.

B. Two-particle experiments

For the two-particle experiments, the differential equations were solved using the fourth-order Runge-Kutta

	FE	RK4
r_{err}	1.446	4.0

Table I. Estimated convergence rate for the numerical methods 4th-order Runge-Kutta (RK4) and Forward Euler (FE).

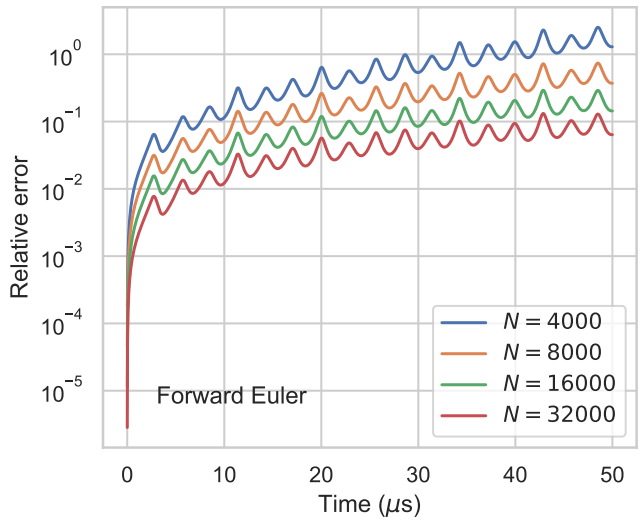

Figure 3. Relative error of the forward Euler method compared to the analytic solution as a function of time. We have included the results from using different number of time steps N over a 50 µs interval.

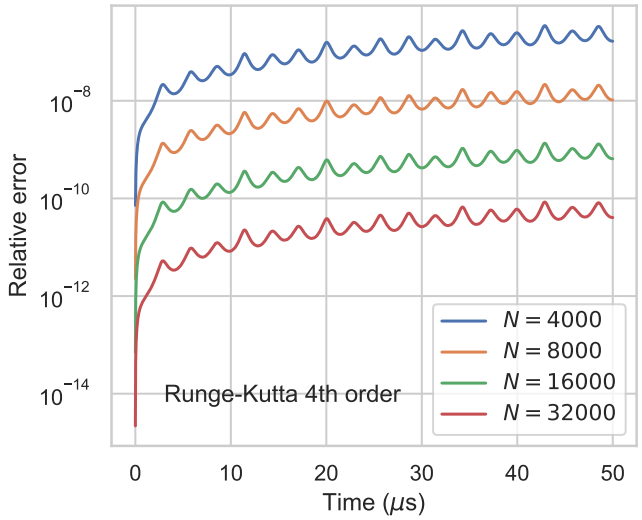

Figure 4. Relative error of the fourth order Runge-Kutta method as a function of time. The error is relative to the analytic solution of a single particle. We have included the results for different number of time steps N along the 50 µs interval.

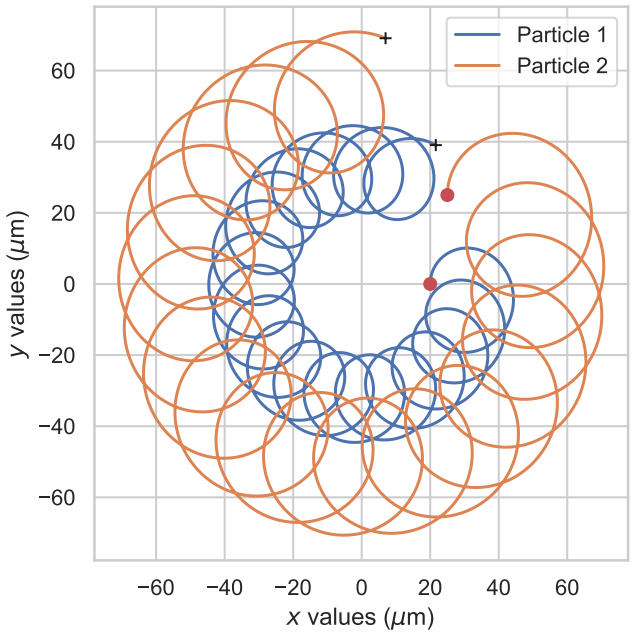

Figure 5. The position trajectory of two particles in the (x, y)-plane from a 50 µs simulation is shown. The initial positions are indicated by the red marker, and the final positions are indicated by the black cross. Here, there was no Coulomb interaction between the two particles that were simulated.

method with time step size of $dt = 0.001$ µm. Of the two particles in the Penning trap, one particle had initial position $(20, 0, 20)$µs and velocity $(0, 25, 0)$µm/µs. We again refer to this as Particle 1. The other particle had initial position $(25, 25, 0)$µs and velocity $(0, 40, 5)$µm/µs. We refer to this as Particle 2. We simulated the particles in the Penning trap for 50 µs.

1. *No particle interactions*

First, we did the numerical experiment without including particle interactions. In other words, we did not include the Coulomb interaction between the particles when computing the force acting on the individual particles. We then plotted the trajectories of the two particles. In Figure 5, we have plotted the trajectory of the particles in the (x, y)-plane. In Figure 6, we have plotted the trajectory of the particles in three-dimensional space. We also plotted the phase space in the x- and z-directions for both particles. In Figure 7, we have plotted the trajectories of the particles in the (x, v_x)-plane. In Figure 8, we have plotted the trajectories of the particles in the (z, v_z)-plane.

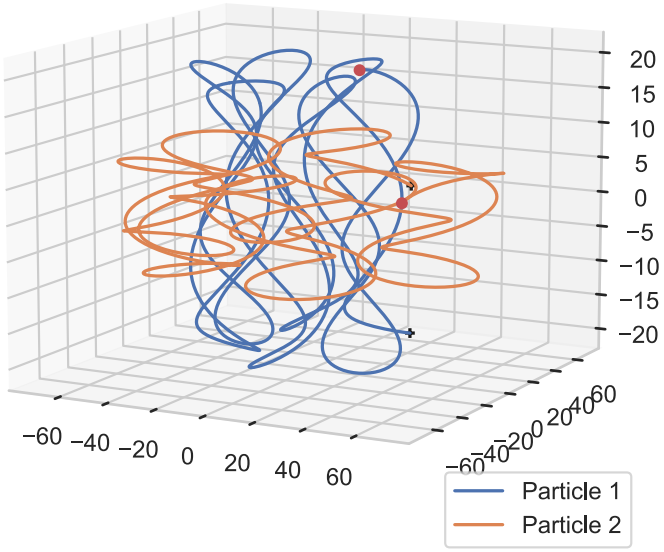

Figure 6. The trajectory of two particles in (x, y, z)-space, where particle interaction was not included in the simulation. We simulated the particles for 50 µs. The red dots indicate the initial positions of the particles, while black crosses mark the final positions.

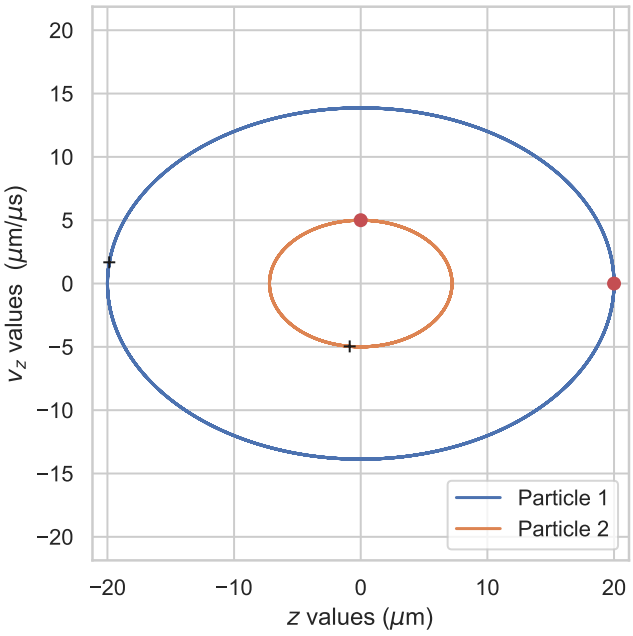

Figure 8. Phase space of two particles with no Coulomb interaction. The plot shows the positions and velocities in the z-direction. The particles were simulated for 50 µs. The red dots mark the initial positions of the particles, and the black crosses mark the final positions ans velocities.

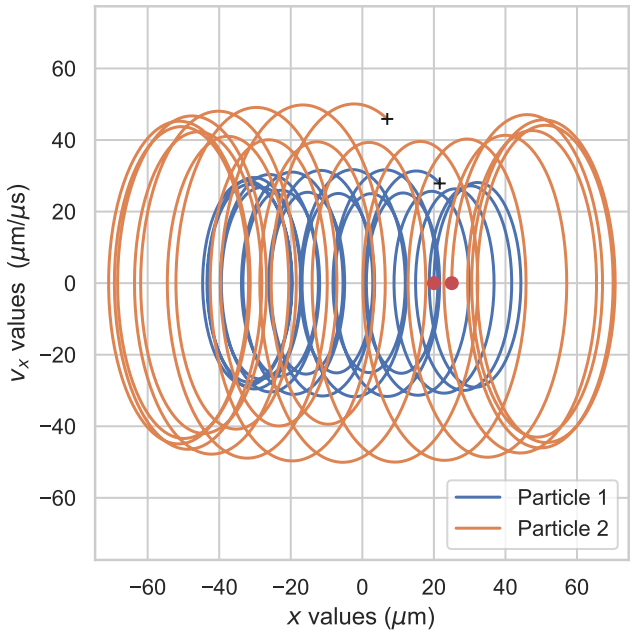

Figure 7. Phase space of two particles simulated over 50 µs without Coulomb interactions. Here we have plotted the positions and velocities in the x-direction. The red dots mark the initial positions and velocities, and the black crosses mark the final positions and velocities.

2. *With particle interactions*

We again simulated Particle 1 and Particle 2 in a Penning trap, but we included Coloumb interactions in the simulation. The trajectory of the particles in the (x, y)-plane can be seen in Figure 9. We also plotted the trajectory in three-dimensional space, see Figure 10. Finally, we plotted the phase space for each particle. In Figure 11 we have plotted the trajectory of the particles in the (x, v_x)-plane, and in Figure 12 we have plotted the trajectory in the (z, v_z)-plane.

C. Time-dependent electric field

We simulated a system of 100 randomly initiated particles in the Penning trap. For these experiments, we applied a time-dependent electrical field, given in (3) to the applied potential. We again used RK4 for finding the numerical solutions, but now with a time step of $dt = 0.05$ µs. We did this to reduce the time needed to complete the numerical experiments. The experiments were more time consuming due to the computational cost of simulating 100 particles with Coulomb interaction.

We explored the behaviour of the system for different amplitudes f and angular frequencies ω_V, to see if we observed any resonance phenomena. In other words, we investigated the fraction of particles that were con-

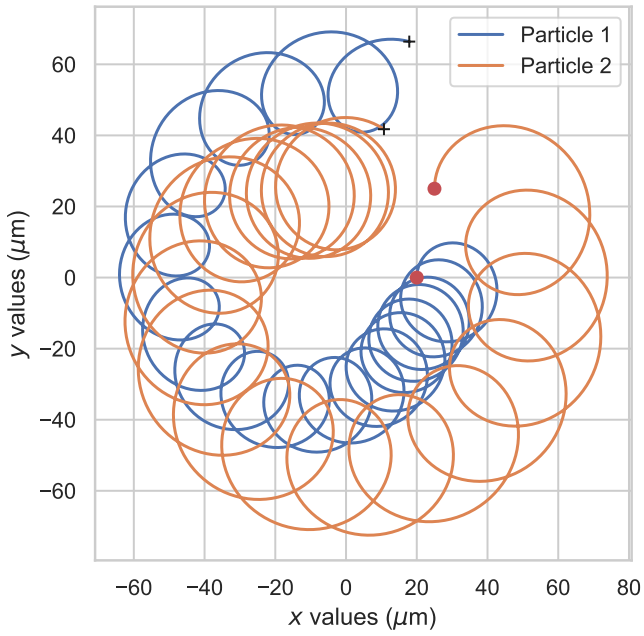

Figure 9. The trajectory of two particles in the (x, y)-plane over a 50 µs simulation is shown. The particles were simulated with Coulomb interaction. The initial positions of the particles are marked by the red dots. The final positions are marked by black crosses.

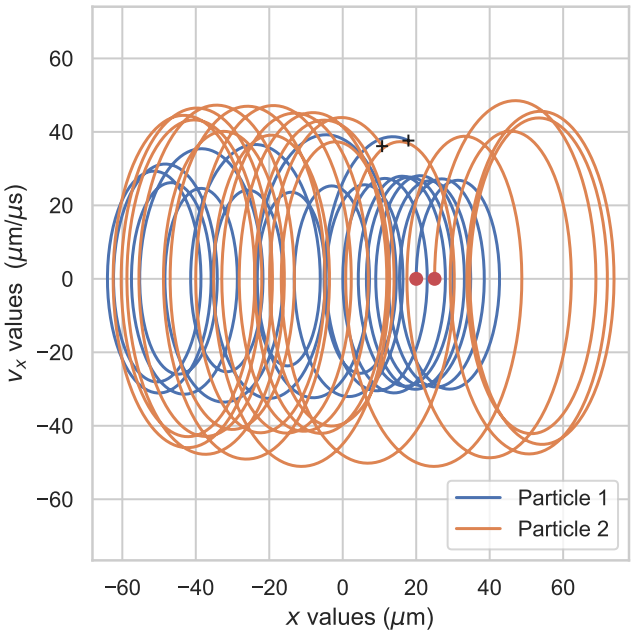

Figure 11. We show the x values and the velocity in the x-direction for two particles with Coulomb interaction. We simulated the particles for a total time of 50 µs. The red dots mark the initial positions and velocities of the particles. The black cross mark the final positions and velocities.

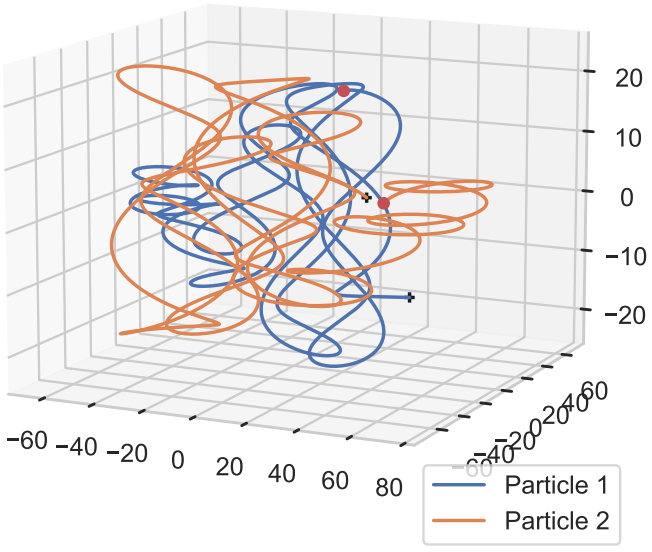

Figure 10. The trajectory in 3D space of two particles in a Penning trap, simulated for 50 µs. The particle interaction was included in the simulation. The red dots mark the initial positions of the particles, and ther black crosses mark the final positions.

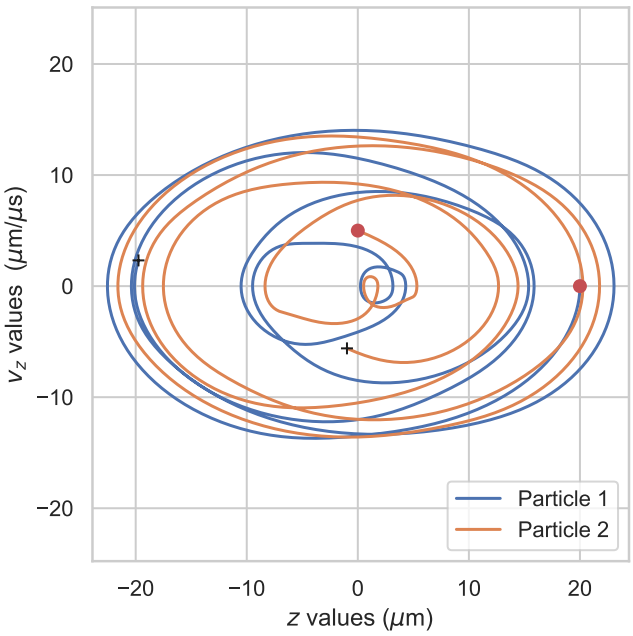

Figure 12. The figure shows the z values and the velocities in the z-direction for two particles. The particles were simulated for 50 µs with Coulomb interactions. The red dots mark the initial positions and velocities of the particles, and the black dots mark the final positions and velocities.

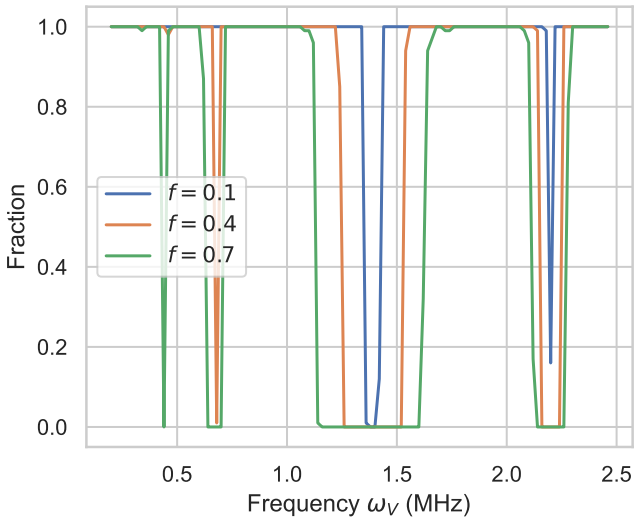

Figure 13. Fractions of particles remaining in the Penning trap after 500 µs. The fractions are plotted as a function of the angular frequency of the time-dependent potential ω_V. We have included the results for amplitudes $f = 0.1, 0.4, 0.7$. We simulated 100 randomly initiated particles.

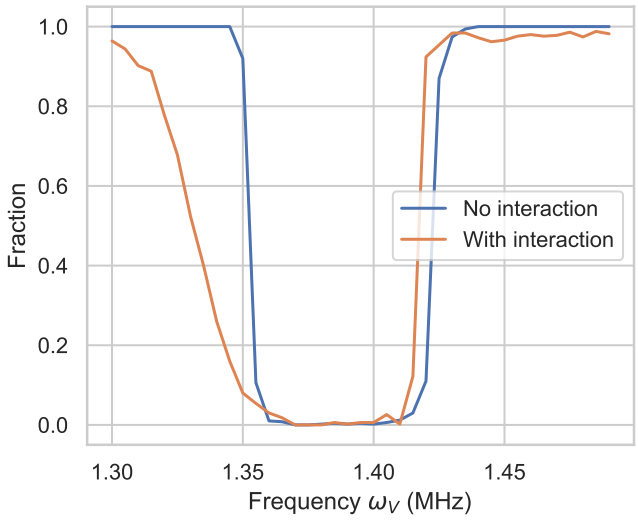

Figure 14. Fractions of particles remaining in the Penning trap after 500 µs. The fractions are plotted as a function of the angular frequency of the time-dependent potential ω_V. The blue line shows the results for 100 particles simulated without Coulomb interactions. The orange line shows the results with Coulomb interactions. Here, the amplitude is $f = 0.1$. The fractions were computed from the average number of particles remaining across 5 experiments.

tained in the Penning trap after 500 µs as a function of the applied frequency. We were interested in exploring frequencies in the range $(0.2, 2, 5)$MHz, with a resolution of 0.02 MHz. In order to efficiently search through such a broad range of frequency values, we did not include particle interactions in the simulation. In searching for resonance frequencies, we used amplitudes $f_1 = 0.1$, $f_2 = 0.4$ and $f_3 = 0.7$. The results of this broad search can be found in Figure 13, where we have plotted the fraction of remaining particles as a function of the frequency, for each of the amplitudes.

Based on the results from this broad search, we further explored a more narrow range of frequency values. Specifically, we looked at $\omega_V \in (1.3, 1.5)$MHz with a resolution of 0.005 MHz. In this case, we simulated the 100-particle system with and without Coulomb interactions. We completed 5 such experiments, and computed the average fraction of particles remaining in the Penning trap for each frequency. The results of the narrow search of resonance frequencies with and without particle interactions can be seen in Figure 14. Here, we used an amplitude of $f = 0.1$.

IV. DISCUSSION

A. Single-particle experiments

With the single-particle experiment, we were able to compare the numerical solution to the analytic solution. This allowed us to estimate the error of the numerical methods. The Euler-Cromer method has the advantage of being a simple algorithm that is easy to implement, but since it has a first-order global error, very small step sizes might be required to get satisfactory results. By comparison, RK4 is a fourth-order method, which means that we can get more accurate results at the cost of implementing a more complex algorithm. We see that the FE method has a large relative error for $N = 4.000$. At the end of the simulation, it misses the true value by around 130%, and even when we do 8 times as many time steps ($N = 32.000$), the error is nearly 6.4% of the true value. By comparison, the relative error of the RK4 method remains small even when we use $N = 4.000$ time steps, at most missing the true value by $1.7 \cdot 10^{-5}$%. As we do not experience that there is a significant cost in terms of computational time needed with using RK4, this is clearly the best choice of algorithm for doing the numerical experiments. The estimated rate of convergence of the two algorithms presented in Table I show that the RK4 error rate agrees with what is expected. The Euler-Cromer error rate is slightly larger than expected. This is a first-order method, but we estimate the error to converge at a rate 1.446.

B. Two-particle experiments

With the two-particle experiment, we looked at how the Coloumb interactions affected the trajectory of the particles in the Penning trap. We observed that with-

out Coulomb interactions, the particles moved in a slow orbital motion about the z-axis while spinning in small loops, see Figure 5 for visualization. From the phase space in Figure 7, we again see that the particles move in circular, "looping" motion along the x-axis, with oscillating velocity. The observed trajectory of each particle agrees with what we would expect to see if the particle was alone in the trap. In the z-direction, the particle trajectories resembled that of a simple pendulum, harmonically oscillating between the extreme values in the z-direction. The movement was stable and periodic, which can be seen clearly from the phase space in Figure 8. These observations agree with what we expect, as the Lorentz force is the only force acting on the particles. The electrical field causes the particles to oscillate periodically along the z-axis. The magnetic field prevents the particles from escaping in the (x, y)-plane, causing the circular orbit about the z-axis to occur.

When Coloumb interactions are included in the simulation, we see that the particles no longer move periodically along the z-axis, and their trajectories become unpredictable. From Figure 9, we see that the trajectory is no longer centered around the z-axis, indicating that the particles "push" each other in different directions. In Figure 12 we see that the simple harmonic motion along the z-axis is no longer present. It is hard to predict exactly how particle interactions will affect the trajectories, but it is not surprising that the overall behaviour of the system is less periodic and stable. The Coloumb force that the particles exert on each other will cause them to repel, effectively perturbing their otherwise periodic trajectories in the z-direction, as well as the stable, orbital motions in the (x, y)-plane.

C. Time-dependent electric field

We introduced a time-dependent electric field to our Penning trap system, and simulated 100 randomly initiated particles. We then explored a range of frequencies and amplitudes for the time-dependent field, to see if we observed resonance phenomena. Resonance phenomena can occur in periodic and quasi-periodic systems when we periodically apply a force that resonates with the system's natural frequencies [6, Ch. 3]. In the case of the Penning trap, a periodic time-dependent electric field can cause the particles in the system to oscillate along the z-axis with greater amplitude, eventually making the particle leave the Penning trap entirely.

We initially simulated a Penning trap with 100 particles that did not interact, in order to do an efficient and broad search for resonance frequencies. For $\omega_V \in (0.2, 2.5)$MHz, we found several regions that indicated resonance. With amplitude $f = 0.1$, the most prominent resonance phenomena occurred for values in the range $\omega_V \in (1.35, 1.4)$, and the region of resonance frequencies increased with greater amplitude. In Figure 13 we see that in this region, the fraction of particles remaining after 500 µs is zero or close to zero. There are also other regions that indicate resonance, although these are less prominent, particularly with smaller amplitude values. The fact that the frequency region increases with amplitude is sensible. With larger amplitudes, the electric field changes more with time, causing a greater change in the motion of the particle along the z-axis.

After completing the broad search, we did a more fine-grained search for frequencies in the range $\omega_V \in (1.3, 1.5)$MHz. Coulomb interactions were included in the experiments, to see how they affected the resonance phenomena. Because the particles are randomly initiated, we performed five such experiments and computed the average fraction of remaining particles for each of the tested frequencies, to get better estimates. Figure 14 shows that the region of resonance frequencies for a system without interaction appears sharply around $\omega_V \in (1.35, 1.42)$MHz. There is a significant fraction of particles that escape the penning trap outside this region when particle interactions are included. This might be due to the fact that when the particles interact, their motion becomes less periodic and stable, which affects their sensitivity to resonance. We also observe that when we include particle interaction, the resonance phenomena does not occur at frequencies larger than 1.415 MHz (for frequencies included in this narrow search). We also note that when there is particle interaction, there seems to be a small fraction of particles that escape the Penning trap outside the frequency region for $\omega_V > 1.415$MHz as well. When there is no particle interaction and no resonance, all the particles tend to remain in the Penning trap after 500 µs. This difference might be because particle interactions introduce greater variance in the system, causing the particle trajectories to behave less predictably.

V. CONCLUSION

We studied the movement of charged particles in an ideal Penning trap, simulating the electric and magnetic fields set up by the trap itself, as well as the fields induced by the particles interacting with each other though the Coulomb force. We saw that for the case of non-interacting charged particles, their movement in the (x, y)-plane traces circular patterns while orbiting a central point. When we introduced the Coulomb force in our model, the two particles began to disturb each other, causing unstable and unpredictable movements.

We compared our numerical models using both the forward Euler and fourth-order Runge-Kutta methods with an analytically calculated specific solution, and found that the error of the FE method was larger than the error of the RK4 method by several factors, even for small time steps, thus indicating that the RK4 method is much more efficient for solving the differential equations. We estimated that the error of the RK4 method converged at a rate of 4.0, while FE converged at a rate of 1.446.

In order to examine the resonance of the system we ran

simulations for several angular frequencies ω_V and plotted the amount of particles remaining in the Penning trap after 500 µs. This allowed us to identify the resonance frequencies of the system by looking at the wavelength regimes where the most particles had escaped the Penning trap. We observed resonance for frequencies between $\omega_V \in (1.35, 1.4)$. We also observed a wider range of frequencies when increasing the amplitude. in the amplitude f broadened the regime of each resonance frequency. When particle interactions were included, a fraction of particles escaped the Penning trap outside this region as well.

[1] A. Kvellestad, FYS3150/4150: Project 3, https://anderkve.github.io/FYS3150/book/projects/project3.html (2022), accessed 19.10.22.
[2] K. Blaum, Y. N. Novikov, and G. Werth, Contemporary Physics **51**, 149 (2010).
[3] A. Kriesch, File:penning trap.svg [internet], https://en.wikipedia.org/wiki/File:Penning_Trap.svg (2006), [Accessed 21.10.22].
[4] P. Scherer, *Computational Physics: Simulation of Classical and Quantum Systems*, Graduate Texts in Physics (Springer International Publishing, 2017).
[5] M. Hjorth-Jensen, *Computational Physics: Lecture Notes Fall 2015* (Department of physics, University of Oslo, 2015).
[6] A. Vistnes, *Physics of Oscillations and Waves: With use of Matlab and Python*, Undergraduate Texts in Physics (Springer International Publishing, 2018).

Appendix A: Derivations

1. The equations of motion

Knowing the force acting on each particle, we can find the equations of motion in all three dimensions $\mathbf{r} = (x, y, z)$, beginning from the general expression for Newton's second law

$$\sum_i \mathbf{F}_i = m\ddot{\mathbf{r}}, \tag{A1}$$

where m is the mass of the particle and $\ddot{\mathbf{r}} \equiv d^2\mathbf{r}/dt^2$ is the double time derivative of the position. We insert the Lorentz force equation (6) and rewrite Newton's second law as

$$q(\mathbf{E} + \mathbf{v} \times \mathbf{B}) = m\ddot{\mathbf{r}}. \tag{A2}$$

Since the electric field is related to the electric potential through equation (1), we have that

$$q(-\nabla \mathbf{V} + \mathbf{v} \times \mathbf{B}) = m\ddot{\mathbf{r}}.$$

When we expand the expression for each of the three directions $\mathbf{r} = (x, y, z)$ it gives us

$$\begin{aligned}
m\ddot{x} &= q\left(-\frac{\partial V}{\partial x} + v_y B_z - v_z B_y\right) \\
m\ddot{y} &= q\left(-\frac{\partial V}{\partial y} + v_z B_x - v_x B_z\right) \\
m\ddot{z} &= q\left(-\frac{\partial V}{\partial z} + v_x B_y - v_y B_x\right).
\end{aligned}$$

This can be further written as

$$\begin{aligned}
m\ddot{x} &= q\left(\frac{V_0}{2d^2}2x + \frac{dy}{dt}B_0 - 0\right) \\
m\ddot{y} &= q\left(\frac{V_0}{2d^2}2y - 0 + \frac{dx}{dt}B_0\right) \\
m\ddot{z} &= q\left(-\frac{V_0}{2d^2}4z + 0 - 0\right).
\end{aligned}$$

We define the constants

$$\omega_0 = \frac{qB_0}{m}, \tag{A3}$$

XXX (where $\omega_0 > 0$ because frequency can't be negative) and

$$\omega_z^2 = \frac{2qV_0}{md^2}, \tag{A4}$$

which lets us express the equations of motion of a particle in all three dimensions as

$$\ddot{x} - \dot{y}\omega_0 - \frac{1}{2}\omega_z^2 x = 0 \tag{A5}$$

$$\ddot{y} + \dot{x}\omega_0 - \frac{1}{2}\omega_z^2 y = 0 \tag{A6}$$

$$\ddot{z} + \omega_z^2 z = 0. \tag{A7}$$

2. The general solutions of the equations of motion

The general solution for (A7) can easily be found if we assume a solution on the form $z = e^{\lambda t}$, where λ is a constant. Inserting this into (A7) gives us

$$\lambda e^{\lambda t}(\lambda^2 + \omega_z^2 \lambda) = 0,$$

which has roots $\lambda_1 = 0$ and $\lambda_2 = -\omega_z^2$. Therefore, the general solution to (A7) becomes

$$z(t) = A + Be^{-\omega_z^2 t}. \tag{A8}$$

The general solutions to the coupled equations (A5) and (A6) are a bit more complicated to find and require the use of a complex function $f(t) = x(t) + iy(t)$ in order to combine them into one differential equation. We use $f(x)$ this to solve (A5) + (A6), which gives us

$$\begin{aligned}
(\ddot{x} + \ddot{y}) + \omega_0(-\dot{y} + \dot{x}) + (-\frac{1}{2}\omega_z^2(x - y)) &= 0 \\
(\ddot{x} + \ddot{y}) + \omega_0(\dot{x} - \dot{y}) - \frac{1}{2}\omega_z^2(x + y) &= 0 \\
\ddot{f} + i\omega_0 \dot{f} - \frac{1}{2}\omega_z^2 f &= 0,
\end{aligned} \tag{A9}$$

where (A9) is (A5) and (A6) expressed as a single differential equation with the general solution

$$f(t) = A_+ e^{-i(\omega_+ t + \phi_+)} + A_- e^{-i(\omega_- t + \phi_-)}, \tag{A10}$$

where ϕ_+ and ϕ_- are constant phases, A_+ and A_- are positive amplitudes and $\omega_\pm$ is defined as

$$\omega_\pm = \frac{\omega_0 \pm \sqrt{\omega_0^2 - 2\omega_z^2}}{2}. \tag{A11}$$

The physical coordinates are then found as $x(t) = \mathrm{Re}\{f(t)\}$ and $y(t) = \mathrm{Im}\{f(t)\}$. In order to find a bounded solution (i.e. a solution where $|f(t)| < \infty$ when $t \to \infty$) for the movement in the xy-plane, we need to put constraint on the values for ω_0 and ω_z. Knowing from (A11) that $\omega_\pm \in \mathbb{R}$ in order to make sense physically, we can see that a bounded solution must have $\omega_0^2 - 2\omega_z^2 > 0$. Therefore we know that $\omega_0 > \sqrt{2\omega_z^2}$.

Inserting our expressions for (A3) and (A4) into this relation we get that

$$\begin{aligned}
\omega_0 &> \sqrt{2\omega_z^2} \\
\frac{qB_0}{m} &> \sqrt{\frac{4qV_0}{md^2}}
\end{aligned}$$

which we can separate into the Penning trap parameters (B_0, V_0, d) and the particle properties (m, q), thus constraining the relation between them.

$$\left(\frac{qB_0}{m}\right)^2 > \frac{4qV_0}{md^2}$$
$$\frac{B_0^2 d^2}{V_0} > \frac{4m}{q} \tag{A12}$$

3. Upper and lower bounds

We can find the upper and lower bounds on the particle's distance from the origin in the xy-plane by rewriting the general solution of the equations of motion in the xy-direction (A10) as

$$f(t) = A_+ \cos(\omega_+ t + \phi_+) - iA_+ \sin(\omega_+ t + \phi_+) + A_- \cos(\omega_- t + \phi_-) - iA_- \sin(\omega_- t + \phi_-).$$

Remembering that the physical coordinates $x(t)$ and $y(t)$ are found by taking respectively the real and imaginary part of the general solution, we have

$$x(t) = A_+ \cos(\omega_+ t + \phi_+) + A_- \cos(\omega_- t + \phi_-)$$
$$y(t) = -[A_+ \sin(\omega_+ t + \phi_+) + A_- \sin(\omega_- t + \phi_-)].$$

We can define the radius

$$R = \pm\sqrt{x^2(t) + y^2(t)},$$

for which we can insert for $x(t)$ and $y(t)$ and use some trigonometric identities to show that

$$R = \sqrt{A_+^2 + 2A_+A_- \cos\left[(\omega_+ t + \phi_+) - (\omega_- t + \phi_-)\right] + A_-^2}.$$

We see that the maximum value for this expression is when the cosine term equals 1, and, likewise, the minimum value is when the cosine term equals -1. Therefore we have that

$$R_+ = \sqrt{(A_+ + A_-)^2}$$
$$R_- = \sqrt{(A_+ - A_-)^2},$$

which shows us that the upper and lower bounds on the particle's distance from the origin are given as:

$$R_+ = A_+ + A_- \tag{A13}$$
$$R_- = |A_+ - A_-|. \tag{A14}$$

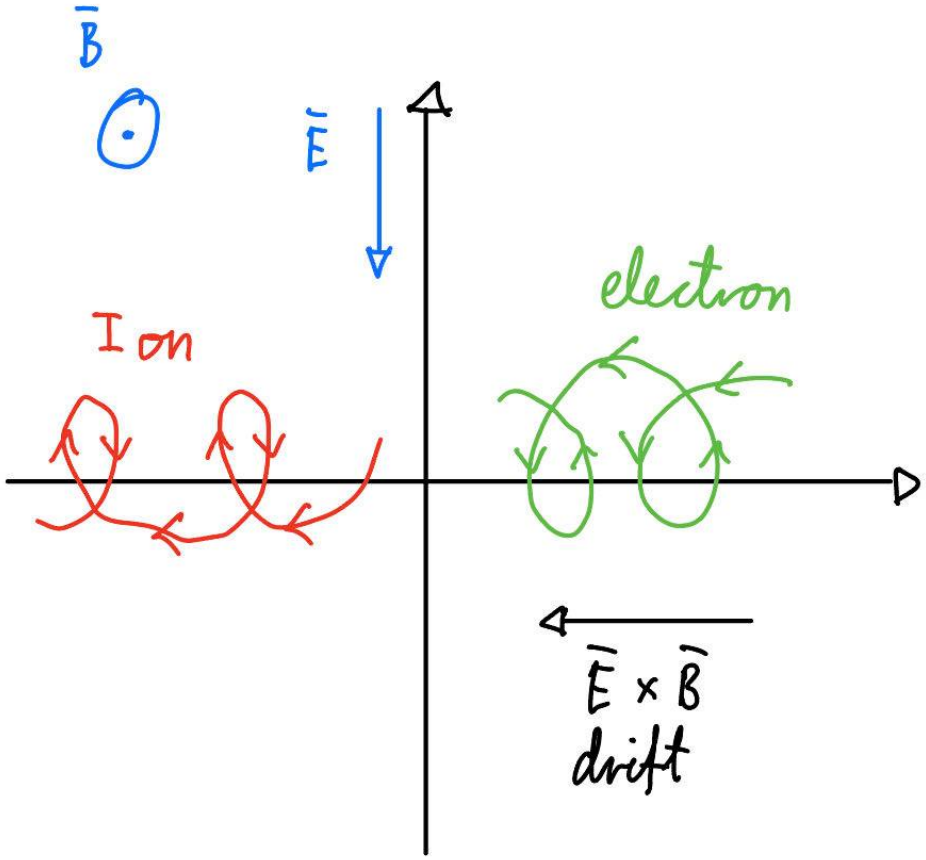

Figure 15. Charged particle motion in a static electric and magnetic field. The greed path represents an electron and the red path an ion. Magnetic field goes into the paper and the electric field points downward, perpendicular to the magnetic field.